# Multiscale Modeling of Permittivity of Polymers With Aging: Analysis of Molecular Scale Properties and Their Impact on Electrical Permittivity

Simone Vincenzo Suraci, *Member, IEEE*, Xavier Colin, and Davide Fabiani, *Senior Member, IEEE*

*Abstract*—This work presents an innovative model for the derivation of permittivity evolution of polyethylene (PE)-based materials with aging. First, the derivation of the microscale contributions to the real permittivity of methylene unit [constitutive repetitive unit (CRU) of PE] and its oxidation products, that is, ketones and hydroperoxides, in the solid state is presented. Then, a chemical kinetic model is recalled predicting the concentration, under proper hypotheses, of the oxidized species created during polymer aging. The proposed model combines the concentrations of methylene unit and its oxidation products with the respective contribution to permittivity, providing the trend of permittivity of polymer with aging. Results depict good agreement with the experimental data, validating the model.

*Index Terms*—Aging, kinetic model, permittivity, polarizability.

## I. INTRODUCTION

**D**UE to the rising demand for energy and the need of delivering this energy over long distances, research on insulating polymeric materials for high-voltage power cables experienced a very fast development. The key properties to be considered for extruded cable design are electrical conductivity ($\sigma$) and permittivity ($\varepsilon$). This latter is one of the key properties of the material and it provides information about the polarization mechanisms occurring inside the dielectric material [1], [2]. These mechanisms are particularly important to understand the behavior of the dielectric material under an applied electric field. Similar to mechanical properties, electrical properties are affected by the microscopical characteristics of a material. When it comes to permittivity, the microscale properties of interest are the polarizability and the volume of the molecules the material is made up of [2]. These quantities are usually obtained using molecular simulation software. Due to the high number of chemical units inside the polymer chain, the computational effort is often very high, and supercomputers are typically used for calculation [3], [4]. The recent advances in the study of first-principles calculations via density functional theory (DFT) with periodic boundary conditions resulted in faster calculations for simple polymeric materials, such as polyethylene (PE) [3]–[5].

Clausius and Mossotti paved the way for the discovery of a relationship between molecular microscopical properties and macroscopical permittivity. In diluted systems, for example, gases, the Clausius–Mossotti (CM) equation is valid only if the intermolecular interactions are ignored. When applied to solids, the equation can lead to incorrect estimations of the dielectric constant, since it neglects important properties such as molecular surface size and orientation. Moreover, the CM equation is not explicitly dependent on the internal electric field of the molecules $E_i$ due to the introduction of the so-called "uniform polarization hypothesis by Mossotti and Lorentz" [2]. $E_i$ is different from the external electric field $E$, since it represents the action of all the charges on a single dipole, this latter is excluded [3]. It is evident that the internal electric field is not easily derivable from theoretical equations, except for some common geometries (e.g., spherical charge displacement).

Furthermore, the properties of polymeric materials may change over time due to aging. This latter, in low-voltage cable systems, is mainly caused by environmental stresses, for example, heat and radiation which may promote various phenomena like oxidation, chain scissions, and crosslinking. The oxidation process results in the formation of new species (e.g., ketones, carboxylic acids, esters, etc.) along the polymer chain, which can significantly alter the polymer properties even at very low concentrations. Up to now, the determination of the permittivity values of degradation species has very limited literature, despite their importance and influence on the macroscopical properties. As a matter of fact, permittivity values reported in previous studies are either based on gas state and diluted solutions containing these species [6] or subject to high uncertainties [7]. This gap can be explained by the impracticality of validating the results generated by

simulations and models on a fully degraded polymer, as will be discussed in the following.

Different experimental techniques, such as transmission Fourier transform infrared (FTIR) spectroscopy, can be applied to measure the degradation of species within aged polymers [8]. On the other side, several researchers formulated kinetic models [8], [9] trying to quantify the increase of concentration of these oxidized species as a function of the aging time and aging conditions. As expected, the higher the accuracy, the bigger the computational effort for the resolution of the kinetic equations. Therefore, semi-empirical models are often used to evaluate these species, but they have narrow applications related to specific polymers and aging conditions.

Once the aging conditions are known, the possibility of linking available kinetic models with the permittivity of unaged polymer and its degradation products opens the possibility of assessing the evolution of permittivity with aging time. Specifically, the results from the model could be compared with those from experiments, validating or contradicting the model.

In this work, the authors present an innovative model aiming at providing an approximate, yet valid approach for the derivation of permittivity of PE-based materials as a function of aging. This is achieved by the coupling of the chemical kinetic model formulated by Hettal *et al.* [8] for PE with the permittivity calculation approach in solids by Natan *et al.* [3]. Once the stress conditions are known, this would allow the assessment and modeling of the polymer permittivity trend with aging.

## II. MICROSCALE PROPERTIES OF MOLECULAR CLUSTERS

### A. Polarizability

*1) Theoretical Background:* The computational effort for the calculation of polarizability $\alpha$ may be significantly reduced under the proper hypothesis. This quantity is to a good extent an additive property; thus, the polarizability can be calculated from a sum of transferable atomic or bond contributions [10], [11]. However, perfect additivity can only occur if the subunits of the same type are noninteracting, which is not the case for atom groups in molecules. Indeed, the presence of chemical bonds inside the molecule brings to the different displacement of charges which modifies the polarizability of the bonded atom with respect to its un-bonded form. In addition, if an electric field is applied to the molecule, the atomic-induced dipole moment may arise as reported in [10].

In order to overcome this complexity, various models based on the additivity approach were proposed in the literature. These methods are, in general, successful in reproducing the molecular mean polarizability [11]. Nonetheless, the deviation of simulated data obtained through pure addition of atomic polarizability from experimental ones is usually below 10%. As an example, in the case of urea molecules, the deviation is reported to be ∼8% [10]. This value tends to reach zero if the molecules are sufficiently far away from each other so that the interaction between two adjacent molecules is negligible, as in the case of, for example, very diluted solutions and gases. Jensen *et al.* [10] investigated some species of interest, that is, methane, urea, and hydrogen fluoride, and they
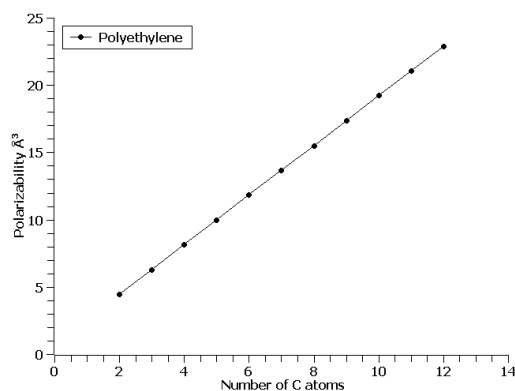


Fig. 1. Polyethylene polarizability values as a function of the number of carbon atoms in the chain.

quantified the minimum distance between molecules beyond which intramolecular interaction may be considered negligible. However, it is not possible to obtain a unique value valid for all the species, since it is deeply influenced by the considered molecular (e.g., dipolar momentum) and matrix (e.g., density) properties.

In the case of dense matter, for example, solids, Natan *et al.* [3] found very good accordance between simple addition and different simulation methods as DFT for polarizability calculations of aromatic molecules. These species are apolar molecules, hence the intermolecular forces may be reduced to the matrix properties of the considered matter. As a confirmation, the same authors claim that the addition approach was successfully applied to the apolar alkyl chain monolayers which can be considered a good structural model for PE chains.

*2) Simulation Approach:* In this work, the additional approach is used as it is considered a good approximation for the calculation of polarizability of dense solid matter. The values of polarizability $\alpha$ are calculated through the chemical simulation software ChemAxon Marvin v.21.8 and Avogadro [12]. As known, PE chains may have different lengths and arrange themselves into ordered structures, that is, crystals. As a first attempt, the authors neglect the morphological arrangement of these species, considering that the PE chain polarizability is given by the sum of polarizabilities of the constitutive repetitive units (CRUs) (e.g., methylene unit $-CH_2-$ in the case of unaged PE) only. The negligence of the contribution of the methyl termination groups ($-CH_3$) is acceptable in the case of long chains, due to the reduced impact of the additional hydrogen atom on the global polarizability, as will be discussed in the following. Moreover, these macromolecules are considered stand-alone so that the intermolecular interactions can be neglected, and the additive approach may be properly applied.

*3) Simulation Results and Discussion:*

*a) Application to polyethylene:* As the chain length of PE is not constant and not *a priori* defined, a parametric study considering PE with different chain lengths was performed (see Fig. 1) aiming at assessing the contribution of a single CRU.
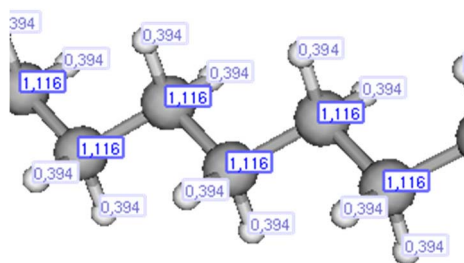
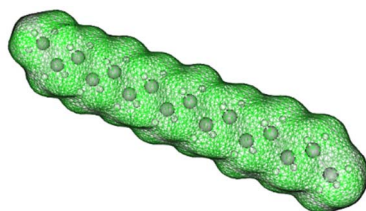Fig. 2. Polyethylene chain with atomic polarization values.



Fig. 3. Charge displacement for polyethylene chain.

Fig. 1 reports the variation of the polarizability value, obtained through Marvin Chemaxon, as a function of the number of carbon atoms in the PE chain. From this analysis, a linear increase of polarizability with the chain length is shown, confirming the suitability of the introduced hypotheses for the application of the additivity approach. Moreover, by dividing the molecular value by the number of carbon atoms inside the simulated macromolecule, it is possible to derive that the average contribution of a single $-CH_2-$ group on the global polarizability is constant and it is $\sim$1.9 Å$^3$.

The same value can be obtained considering the atomic polarizabilities (see Fig. 2). In this case, the polarizability of the $-H_2-$ group is given by the sum of the different contributions of the atoms ($\sim$1.9 Å$^3$).

Given the constant variation of polarizability with chain length (additivity hypothesis), it is possible to reduce the simulation computing time, simulating small molecules in place of very long polymeric chains. The Chemaxon Marvin software platform may provide the charge displacement of the simulated molecule which is of great interest for the evaluation of, for example, dipolar momentum. Nonetheless, PE is a nonpolar molecule due to the similar values of electronegativities of the two-component atoms (carbon and hydrogen) (see Fig. 3). As a result, the charge displacement is homogenous throughout the simulated carbon bone and the dipole moment results are zero.

*b) Application to degradation products:* It is known that the main degradation mechanism inside an organic material is oxidation. Literature is plenty of studies explaining the oxidative reactions taking place inside common polymers, for example, PE and polypropylene (PP) [8], [9], [13], [14]. Even in the case of an oxidized polymer, the resulting chain is made up of CRUs, as reported in Fig. 4 for hydroperoxides (POOH). In this work, the performed analyses consider some of the most common oxidation degradation products, namely hydroperoxides, alcohols, ketones, aldehydes, carboxyl acids, and esters.
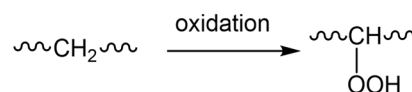


Fig. 4. Oxidation products for methylene. Case of hydroperoxide.

TABLE I

SOFTWARE SIMULATION. POLARIZABILITY VALUES FOR OXIDATIVE DEGRADATION PRODUCTS INSIDE POLYETHYLENE

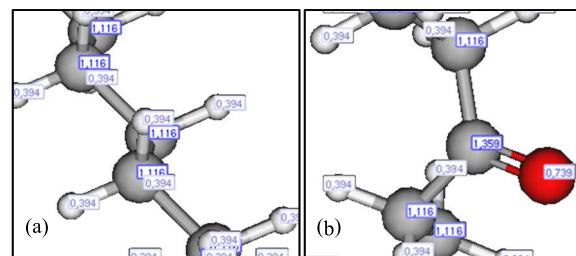| Species name | Species chemical formula | Polarizability (Å$^3$) | Dipole moment (D) |
|---|---|---|---|
| Methylene | $-CH_2-$ | 1.9 | 0 |
| Hydroperoxides | —CH— OOH | 3.52 | 1.65 |
| Alcohol | —CH— OH | 2.7 | 1.7 |
| Ketone | —C— ‖ O | 2.1 | 2.9 |
| Aldehyde | —C— H, O | 2.5 | 2.9 |
| Carboxyl acid | —C— OH, O | 3.15 | 2.27 |
| Ester | —C—O— ‖ O | 2.93 | 2.1 |



Fig. 5. (a) Atomic polarizability of unoxidized and (b) oxidized polyethylene chain with a ketone group.

Under the hypotheses presented in the previous section, it is possible to consider the contribution of the degradation products to the polymer polarizability through a parametric study. As a result, constitutive CRU polarizabilities and dipole moments, obtained through the Marvin Chemaxon platform, for the different degradation groups are reported in Table I.

From this table, it is possible to notice that the presence of oxygen molecules raises all the analyzed electrical microscopical quantities. In particular, as polar species, oxygen increases the polarizability of the molecule and, consequently, the electrical response of the resulting chain once subjected to an external electrical field. Indeed, the modification of the repetitive unit structure, that is, the introduction of –OH or multiple bonds, raises the atomic polarizability of the carbon atom and, consequently, the polarizability of the global molecule. As an example, in the case of ketones, the presence of the double bond with oxygen causes the atomic polarizability of carbon to raise to 1.36 Å$^3$ [see Fig. 5(b)], with respect to the PE chain value of 1.12 Å$^3$ [see Fig. 5(a)].

The increase in polarizability is not the same among the considered species. As expected, molecular polarizability and

TABLE II
COMPARISON TABLE BETWEEN POLARIZABILITIES OBTAINED THOUGH
SIMULATION SOFTWARE AND THE ADDITIVITY APPROACH

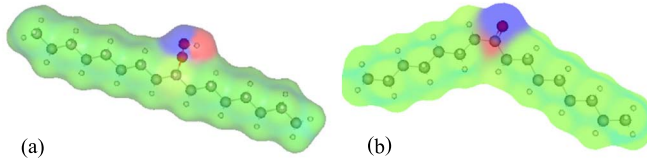| Molecule | Number oxidative species | Polarizability (software) ($Å^3$) | Polarizability (addition) ($Å^3$) | Dev (%) |
|---|---|---|---|---|
| $C_{96}H_{194}$ | - | 178 | 184 | 3 |
| $C_{96}H_{164}O_{15}$ | 15x C=O (ketone) | 188.5 | 187 | 0.7 |
| $C_{96}H_{149}(OH)_{15}$ | 15x C-OH (alcohol) | 201 | 195 | 3 |
| $C_{96}H_{149}(OOH)_{15}$ | 15x COOH (hydroper.) | 212 | 208 | 1.9 |



Fig. 6. Charge displacement. (a) Hydroperoxide. (b) Ketone.

dipolar momentum are higher when two oxygen atoms bond to the polymer backbone, as in the case of hydroperoxides, esters, and carboxyl acids (see Table II).

Let us consider two of the most common degradation species: hydroperoxides (POOH) [Fig. 6(a)] and ketones (C = O) [see Fig. 6(b)]. In the first case, the presence of additional oxygen raises the polarizability, while it decreases dipole moment due to the electronegativity balance between the two oxygen molecules. On the contrary, the ketone group brings to an asymmetric charge displacement which brings to the bending of the PE chain, resulting in a higher dipolar momentum.

To further validate the additive approach for the calculation of polarizability of unaged and oxidized PE chains, macromolecules made up of 96 carbon atoms were simulated through the Marvin platform. The obtained polarizabilities are compared with the ones given by the summation of polarizabilities of constitutive groups (see Table II). From this comparison, it is possible to highlight that very low error dispersion (significantly lower than the 10% initially reported) is present among the obtained values.

### B. Molecular Volumes

*1) Simulation Approach:* The used simulation software allows the calculation of the molecular van der Waals volume. The use of this quantity can be misleading since it is referred to the volume occupied by the molecule if no intermolecular interactions are present. While this can be acceptable inside gases or diluted solutions, it is not the case with solid matter, for example, polymers where strong molecular interaction forces are present, permitting the material cohesion. Molecular volumes, in the case of solids, may be evaluated by means of density, which gives information about the number of molecules inside a reference volume. In other words, this quantity may provide data about the packing of molecules and
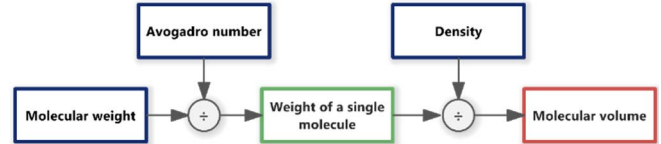


Fig. 7. Schematic of molecular volume calculations.

the macromolecular structure arrangement inside the polymer. As an example, the density of semicrystalline polymers is placed in between the values of density related to the corresponding crystalline (denser) and amorphous (less dense) phases.

Thus, it is evident that molecular volumes obtained through calculations involving density are different from, usually lower than, the theoretical van der Waals volumes.

Nonetheless, the values obtained through density parameters showed to be more realistic delivering good results for the calculation of the real permittivity, as will be seen in Section III. Moreover, as density varies during aging [14], [15], the derivation of density values for oxidized polymers may bring to the definition of molecular volumes of degradation species.

The procedure for obtaining molecular volumes is based on simple chemical calculations [see the diagram in Fig. 7 and (1)] involving molecular weight $M_W$, density $\rho$, and the Avogadro number $N_A$, as in the following equation:

$$\nu = \frac{M_w / N_A}{\rho} \ (m^3).\tag{1}$$

Similar to what was reported for the calculation of polarizability, we consider the unaged PE as made up of the same CRU (–$CH_2$–), which has a molecular weight equal to $M_{CH2} = 14$ g/mol.

The density $\rho$ is usually well known in the case of common polymers, such as PE ($\rho \sim 0.9$ g/cm$^3$). On the contrary, the density values of the degradation species coming from polymer aging are not *a priori* defined and further analysis is required, as reported in [14].

*2) Determination of the Density Changes With Aging:* In the case of semicrystalline polymers, it is possible to consider the relationship reported in (2). The density $\rho$ can be expressed as a function of the densities of its amorphous $\rho_a$ and crystalline phases $\rho_C$ as follows:

$$\rho = V_C \rho_C + (1 - V_C)\rho_a \tag{2}$$

where $V_C$ is the volume fraction of crystals.

According to (2), two causes may be responsible for an increase in $\rho$ during aging.

1) The incorporation of "heavy" atoms such as oxygen into a polymer structure initially contains many "light" atoms (i.e., carbon and hydrogen) [14].
2) The integration of short fragments, coming from chain scission phenomena to crystalline lamellae. This induces a chemicrystallization, that is, thickening of crystalline lamellae and an increase in the crystallinity ratios (i.e., $V_C$), as experimentally observed elsewhere [14].

Thus, (2) relates the increase of density due to aging with the integration of oxidized species along with the macromolecular structure modification.

| Species name | $M_{CRU}$ (g.mol$^{-1}$) | $n_{O2}$ | $Q_{O2}/n_{O2}$ (mol.cm$^{-3}$) | $\Delta\rho_a/Q_{O2}$ (g.mol$^{-1}$) |
|---|---|---|---|---|
| Hydroperoxides | 32 | 1 | 0.061 | 37.33 |
| Alcohol | 16 | 1/2 | 0.061 | 37.33 |
| Ketone | 14 | 1/2 | 0.053 | 70.27 |
| Aldehyde | 15 | 1/2 | 0.057 | 52.71 |
| Carboxyl acid | 31 | 1 | 0.059 | 44.77 |
| Ester | 30 | 1 | 0.057 | 52.71 |

| Species | $\frac{\Delta\rho}{\Delta Q_{O2}}$ (g/mol) | $\rho$ (g/cm$^3$) | Molecular volume (m$^3$) |
|---|---|---|---|
| Methylene | - | 0.912 | 2.58 10$^{-29}$ |
| Hydroperoxide | 55.3 | 4.23 | 1.77 10$^{-29}$ |
| Alcohol | 55.3 | 2.6 | 1.85 10$^{-29}$ |
| Ketone | 75.75 | 2.92 | 1.59 10$^{-29}$ |
| Aldehyde | 64.85 | 2.76 | 1.74 10$^{-29}$ |
| Carboxylic acid | 59.92 | 4.39 | 1.70 10$^{-29}$ |

The density variation given by the introduction of degradation products inside the PE matrix can be written as

$$\Delta\rho = (1 - V_{Cini})\Delta\rho_a + (\rho_C - \rho_{aini})\Delta V_C \quad (3)$$

where $V_{Cini}$ is the value of the fraction of the crystalline phase of the unaged XLPE (37.9%), $\rho_{aini}$ is the density of the amorphous phase of the unaged XLPE (0.85), and $\rho_c$ is the density of the crystalline phase (1.014) [14].

In [14], we verified that the increase in density of the amorphous phase $\Delta\rho_a$ and the increase in crystallinity ratio $\Delta V_C$ of the XLPE matrix during the radio-thermal aging are linear functions of the oxygen consumption $\Delta Q_{O2}$. The first proportionality constant (between $\Delta\rho_a$ and $\Delta Q_{O2}$) can be theoretically determined by assuming the main oxidation products formed in the XLPE matrix (see Table III).

The second proportionality constant can be empirically determined by plotting experimental values for $V_C$ versus the values of $Q_{O2}$. The relationship is given by

$$\Delta V_C = 1.96 \cdot 10^{-1}\Delta Q_{O2}. \quad (4)$$

To quantify the variation of density caused by the presence of degradation products, so that (2) can be applied, some key factors still have to be defined. These values are reported in Table III per each degradation group considered [14]. Finally, it is possible to obtain the density of the degradation product inside a polyethylene matrix by the simple addition:

$$\rho = \rho_{ini} + \Delta\rho. \quad (5)$$

*3) Simulation Results and Discussion:* By applying (2) for the considered degradation products, we can obtain their densities and the corresponding molecular volumes through (1). Focusing on the results reported in Table IV, one can notice values of density that are uncommon for PE-based materials. It is worth recalling that these values are obtained by regression from real values of density of aged PE materials which usually have very little concentration of oxidized products. On the contrary, values obtained in Table IV are referred to as PE chains in which all the hydrogen groups are substituted with the oxidative groups reported in Table III. Obviously, such a material is not obtainable in real conditions, as example, no substitution of hydrogen atoms is possible inside the crystalline phase. Therefore, it is not possible to experimentally verify the density of the oxidized amorphous phase. Results should be validated by the application of the permittivity model and comparison with real values of $\varepsilon$, as will be presented in the following. Even so, as projected,

the degradation species characterized by two oxygen atoms exhibit higher values of density ($\sim$4.3 g/cm$^3$), while it is lower in the case of oxidative species with just one oxygen atom ($\sim$2.7 g/cm$^3$).

As a result, the calculated molecular volumes are lower (down to half) than the values related to the neat PE group. This result is unexpected since the substitution of a small atom, as hydrogen in PE, with a bigger atom, as oxygen, should increase the volume of the considered molecule. This is the case of the van der Waals volumes obtained through the molecular simulation software. On the other hand, as partially described above, the theoretical increase of volume is counterbalanced by, though minor than the effect of, the higher density inside the reference volume. This brings to stronger interaction forces among molecules, which result to be more packed and squeezed, leading to a reduction of their volume in comparison with the theoretical van der Waals one. Similar results may also be seen in the work by Krevelen [7].

## III. MACROSCALE PERMITTIVITY OF POLYMERS

### A. Calculation Approach

The interest in the calculation of the dielectric constant of solid materials encouraged the formulation of innovative methods and approaches. Among those, Natan *et al.* [3] analyzed the properties of polarizability and dielectric constant of nanoscale molecular layers by comparing the calculations coming from the DFT with phenomenological models based on polarizable dipolar arrays.

It is worth recalling that polarization $P$, that is, the induced dipole per unit volume (6) is given by the product between susceptibility $\chi$ and the average internal field in the material $E_i$

$$P = \chi \cdot E_i. \quad (6)$$

For monolayers made up of finite-length monomers, it is possible to write the average internal field as

$$E_i = E - 4\pi P \quad (7)$$

where $E$ is the applied external electric field.

It is possible to approximate that the internal electric field is almost equal to the external one if the distances in-between molecules are big enough to neglect the effect of the electric field related to the polarization of the adjacent molecules. This is the case of, for example, gases and nonviscous liquids (CM model).

In the model by Natan *et al.*'s, the authors reconsider the polarization vector per unit volume (6) introducing a new quantity, the modified susceptibility $\tilde{\chi}$, which permits the writing of the polarization vector as a function of the external electric field $E$. In this way, the modified factor considers the response of the dielectric material under both internal and external electric fields. Namely

$$P = \tilde{\chi} \cdot E. \tag{8}$$

Then, combining (7) and (8), we obtain

$$\chi = \frac{\tilde{\chi}}{1 - 4\pi \tilde{\chi}}. \tag{9}$$

In the case of solids, the term $-4\pi P$ in (7) cannot be removed due to the intermolecular forces taking place inside the material and it should be added inside the CM formula for the calculation of the susceptibility, giving

$$\tilde{\chi} = \frac{\alpha/v}{1 + 8\pi \alpha/3v}. \tag{10}$$

Finally, the dielectric constant may be obtained, in the case of molecular films, as

$$\varepsilon = \frac{1}{2 - \tilde{\varepsilon}} \tag{11}$$

where $\tilde{\varepsilon} = 1 + 4\pi \tilde{\chi}$.

The values of dielectric permittivity given by (11) were proved to be valid for numerous species of polymeric and metallic solids at the base state as reported in [3] and [4].

*1) Modeling Results and Discussion:* After the derivation of the microscopical properties, as reported in Sections II-A and II-B, the application of (11) allows the calculation of the macroscopical permittivity for the simulated repetitive unit species. Results are reported in Table V.

It is worth highlighting that, as expected, the oxidized species exhibit higher values of the resulting real part of permittivity. In particular, higher $\varepsilon$ values are obtained in the case of groups with two oxygen atoms, as already discussed with reference to their polarizability values. Moreover, while it is not feasible to obtain experimental validation for polymer chains made up of oxidized groups only, data for the plain polyethylene show an experimental value $\varepsilon_{\text{exp}}$ ranging between 2.2 and 2.4, which perfectly fits the modeling results reported in Table V.

## IV. PERMITTIVITY CHANGES DURING AGING

### A. Modeling Approach

The increase in the concentration of oxidized polymer chains during aging brings the rise of the real permittivity of the global material. Thus, it is possible to consider the aged polymer as a composite material made up of both unaged and aged repetitive chains. The quantities of these two groups are not easily definable since the aging mechanisms are numerous and, in some cases, can have opposite effects (e.g., chain scissions, crosslinking, and radical recombination). However, the kinetic model presented in [8] and [14], under some hypotheses, permits the definition of the concentration of oxidized polymer species inside the polymer compound with aging. In particular, in this work, the authors consider three degradation species, that is, hydroperoxides, ketones, and

TABLE V
REAL PART OF PERMITTIVITY RESULTS FOR THE ANALYZED CRUs

| Polymer | Species | Modified susceptibility ($\tilde{\chi}$) | Relative permittivity, real part ($\varepsilon$) |
|---|---|---|---|
| **Neat PE** | Methylene | $4.53 \times 10^{-2}$ | 2.32 |
| **Oxidized PE** | Hydroperoxide | $7.46 \times 10^{-2}$ | 16.1 |
| | Alcohol | $6.56 \times 10^{-2}$ | 5.7 |
| | Ketone | $6.47 \times 10^{-2}$ | 5.35 |
| | Aldehyde | $6.51 \times 10^{-2}$ | 5.5 |
| | Carboxylic acid | $7.26 \times 10^{-2}$ | 11.4 |
| | Ester | $7.25 \times 10^{-2}$ | 11.2 |

carboxyl acids, since they are reported to represent $\sim$75% of the total degradation products in aged polymers [14].

Literature reports several approaches for the calculation of the global permittivity for composite materials, usually considering the volume fraction occupied by the inclusions (e.g., fillers) in the lattice. One of the most common is the Maxwell–Garnett equation [16]. However, all these approaches consider the substitution of one species (e.g., polymer) with another one (e.g., fillers), not allowing the use of multiple inclusions.

In this work, the authors propose a new approach that relates the concentration of the different species (e.g., PE matrix, degradation products) and the corresponding permittivities with the global permittivity of the polymeric compound. The obtained results should be then validated by comparing them with experimental ones. As a first attempt, we could consider a linear dependence between the two parameters, namely

$$\varepsilon = \sum_i Y(t)_i \cdot \varepsilon_i \tag{12}$$

where $Y(t)_i$ is the molar fraction of the considered species, calculated through the kinetic model [8], and $\varepsilon_i$ is the real part of permittivity of the species (as in Table V).

Values of the real part of permittivity given by solving (12) for different aging times result to be significantly lower than the one obtained through experimental tests at lab-scale measurable frequencies. The reason for that can be related to the permittivity dependence on frequency. Indeed, the hypotheses considered for the calculation of polarizability (Section II-A) and permittivity (Section III) neglect the contribution of the temperature-dependent polarizations (i.e., dipolar and interfacial polarization), occurring at frequencies lower than $\sim 10^{10}$ Hz. Nonetheless, the contributions of these polarization mechanisms to the real permittivity are minor in the case of nonpolar and nonfilled materials, for example, plain PE where the dipolar momentum is equal to 0 D and the interfaces given by its semicrystalline structure are very few. On the contrary, the dipolar and interfacial polarization mechanisms are prevailing if we introduce polar species inside the polymeric compound, such as during polymer aging. As reported in Section II-A, simulation results claim a very high value of dipolar momentum, up to 3 D (see Table I), which may completely rule the permittivity trend in the dipolar polarization frequency region, raising the $\varepsilon$ value. At the same time, the introduction of different oxidative groups in the polymer matrix enhances the interfacial polarization response.

To consider the impact of the degradation species in the permittivity calculation, we introduce a dipolar enhancement
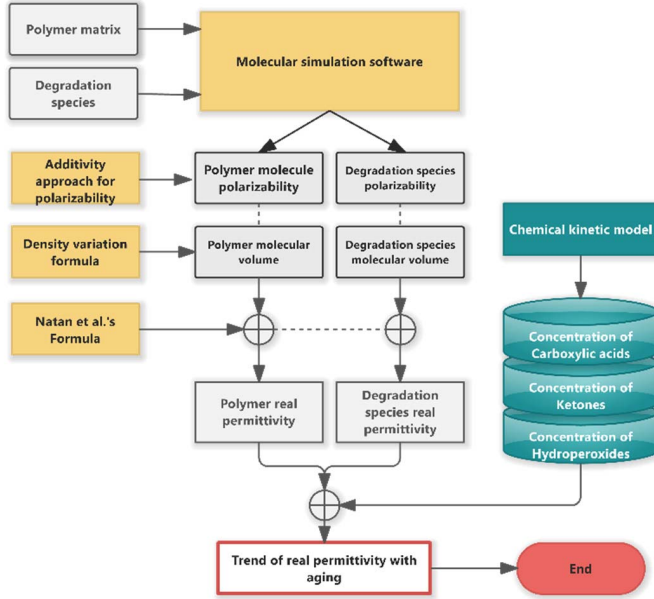
Fig. 8. Schematic of the modeling approach proposed for the calculation of real part of permittivity of solids.

TABLE VI
ACCELERATED AGING CONDITIONS

| Aging type | Aging properties | | | |
|---|---|---|---|---|
| | Dose rate (Gy/h) | Sampling time (h) | Total absorbed dose (kGy) | Temp (°C) |
| Low (LDR) | 7 | 3456 | 120 | 47 |
| Med (MDR) | 66 | 864 | 286 | 47 |
| High (HDR) | 400 | 167 | 334 | 21 |



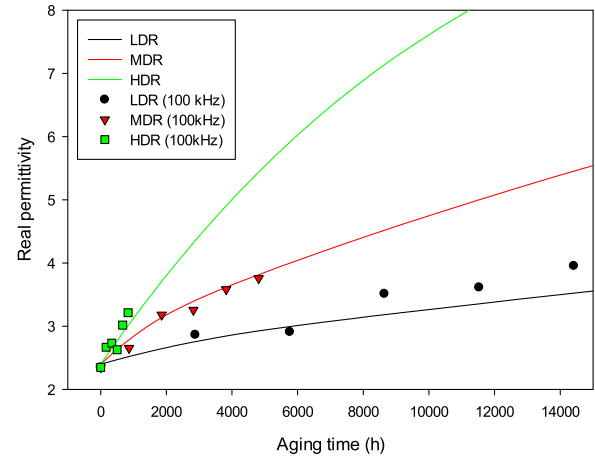Fig. 9. Real part of permittivity as a function of aging time. Solid curves are results coming from the model. Scatter points are experimental data.

factor $\eta$ in (12). This factor applies to the polar species simulating their electrical response at the testing frequency. As a consequence, the proposed index $\eta$ is the function of the chosen frequency and species' electrical properties (e.g., dipolar momentum for the dipolar polarization frequency region).

The frequency chosen for the evaluation of the aging status of polymer is 100 kHz, which was found in our previous works to successfully follow the increase of the degradation products due to aging stresses [15], [17]–[19]. At this stage, $\eta$ is chosen to best fit the experimental data. In the case of the investigated PE, a good tentative value for $\eta$ was found to be equal to 3. Thus, (12) becomes

$$\varepsilon = \sum_i Y(t)_i \cdot \varepsilon_i \cdot \eta_i$$
$$= Y(t)_{PE} \cdot \varepsilon_{PE} + 3 \cdot \sum_i Y(t)_{polar} \cdot \varepsilon_{polar}. \quad (13)$$

The schematic summarizing the proposed modeling approach is reported in Fig. 8.

### B. Simulation and Experimental Results

From the kinetic model presented in [8] and [14], we know that the concentration of degradation species does not linearly increase with aging time. In particular, hydroperoxides are supposed to reach a plateau after a given period of time depending on the aging condition considered. On the contrary, the concentration of ketones and carboxylic acids continues raising throughout the entire aging. Hence, during the first aging period, the increase of oxidative species is very fast, and it slows down once the POOH plateau is reached. Obviously, the velocity of the increasing trend is given by the harshness of the aging conditions and the stronger the aging stresses, the faster the formation of degradation species.

By applying the model proposed in the previous paragraph, we expect that the increasing trend of the real part of permittivity will follow the trend of the degradation species.

In order to validate the proposed model, simulation results are compared to experimental tests performed on a plain XLPE. In this work, we considered a PE crosslinked through the condensation of silanol side groups (Si-XLPE) subjected to three different aging conditions. To accelerate the degradative effects, aging was obtained through the combination of gamma radiation and temperature, as reported in Table VI. Radiation aging was performed by UJV (Rez, Czech Republic) through a $^{60}$Co irradiation source. The permittivity of these materials is evaluated by means of a Novocontrol Alpha Dielectric Analyzer v2.2 operating in the frequency region $10^{-2}$–$10^6$ Hz at 3 $V_{rms}$.

Fig. 9 reports the results obtained by the model and the experimental data. Solid curves, one per each aging condition considered, represent the results acquired by the application of (13) for the different aging conditions and durations considered. Scatter points refer to the experimental data coming from the dielectric analyzer. As it can be seen, very good correspondence between the model and the experimental results is obtained, claiming the effectiveness of the proposed formula for coupling the species concentrations with the corresponding simulated permittivities.

It is worth noting that the model curves (see Fig. 9) follow the expected kinetics trend. Indeed, permittivity values exhibit a steep increase during the first aging period due to the rise of all the degradation species. Then, once the hydroperoxides reach their plateau, the real part of permittivity is ruled by the carboxyl acid and ketone kinetics only. This brings to the change of the increasing pace of $\varepsilon$ with aging time.

### V. CONCLUSION

In this work, a model for the evaluation of the real part of permittivity of solids with aging is proposed and discussed. The model couples the concentration of the species inside the

considered polymer given by the chemical kinetic model with the corresponding permittivity values. These latter ones are calculated through innovative approaches aiming at reducing the computational effort and at ensuring a higher consistency with real values. To achieve so, the authors introduced some simplifying hypotheses for the calculation of molecular polarizability values and assessment of polymer density variations with aging. Nonetheless, the preliminary results presented in this article are promising, delivering realistic permittivity values for neat and aged polymers.

In particular, this work validated the additivity approach for the calculation of microscopical polarizability of molecules inside the material. This allowed the evaluation of the property just by the addition of the different atomic polarizabilities, sensibly reducing the computation effort for the calculation of complex macromolecular structures. On the other side, molecular volumes were obtained by means of a chemical semi-empirical model for density, ensuring more realistic and reliable parameters. These microscopical parameters were used for the calculation of the real part of permittivity for methylene groups and their degradation products (ketones, hydroperoxides, etc.) in the solid state.

The obtained permittivity values were then combined with the real concentration of the different species given by chemical analyses (kinetic model), allowing the formulation of a model which assesses the trend of permittivity of PE with aging, once the stress conditions are known. The proposed equation showed to well fit the experimental results once the dipolar enhancement factor is introduced in the model. This factor is obtained by best fitting with experimental data at the present work since it is the function of the testing frequency and polymer-related characteristics. Indeed, it considers the effect of dipoles and interfaces which are not considered by the computation of molecular polarizability, but they deeply influence the permittivity at testing frequencies.

The presented model would be of particular interest because it would reduce the need for experimental tests on real materials and permit an easier simulation of electrical equipment under testing and operation conditions. Moreover, the lifetime of the polymer may be evaluated once the aging conditions are known, if any end-of-life criterion based on the real permittivity is set for the considered polymer.

Future work on this topic will include the analysis and simulation of permittivity of thermally aged polymers, aiming at further validating the proposed modeling approach.

## ACKNOWLEDGMENT

## REFERENCES

[1] A. Schönhals, "Dielectric spectroscopy on the dynamics of amorphous polymeric systems," Novocontrol, Montabaur, Germany, Appl. Note Dielectr. 1, 1998.

[2] F. Kremer and A. Schönhals, Eds., *Broadband Dielectric Spectroscopy*. Berlin, Germany: Springer, 2003, doi: 10.1007/978-3-642-56120-7.

[3] A. Natan, N. Kuritz, and L. Kronik, "Polarizability, susceptibility, and dielectric constant of nanometer-scale molecular films: A microscopic view," *Adv. Funct. Mater.*, vol. 20, no. 13, pp. 2077–2084, May 2010, doi: 10.1002/adfm.200902162.

[4] H. M. Heitzer, T. J. Marks, and M. A. Ratner, "Computation of dielectric response in molecular solids for high capacitance organic dielectrics," *Accounts Chem. Res.*, vol. 49, no. 9, pp. 1614–1623, Sep. 2016, doi: 10.1021/acs.accounts.6b00173.

[5] M. Unge, C. Törnkvist, and T. Christen, "Space charges and deep traps in polyethylene—*Ab initio* simulations of chemical impurities and defects," in *Proc. IEEE Int. Conf. Solid Dielectr. (ICSD)*, Jun./Jul. 2013, pp. 935–939, doi: 10.1109/ICSD.2013.6619874.

[6] R. L. Smith, S. B. Lee, H. Komori, and K. Arai, "Relative permittivity and dielectric relaxation in aqueous alcohol solutions," *Fluid Phase Equilibria*, vol. 144, nos. 1–2, pp. 315–322, Feb. 1998, doi: 10.1016/S0378-3812(97)00275-6.

[7] D. W. Krevelen, *Properties of Their Correlation With Chemical Structure; Their Numerical Estimation and Prediction From Additive Group contributions*, 3rd ed. Amsterdam, The Netherlands: Elsevier, 1997.

[8] S. Hettal, S. Roland, K. Sipila, H. Joki, and X. Colin, "A new analytical model for predicting the radio-thermal oxidation kinetics and the lifetime of electric cable insulation in nuclear power plants. Application to silane cross-linked polyethylene," *Polym. Degradation Stability*, vol. 185, Mar. 2021, Art. no. 109492, doi: 10.1016/j.polymdegradstab.2021.109492.

[9] K. T. Gillen and R. L. Clough, "A kinetic model for predicting oxidative degradation rates in combined radiation-thermal environments," *J. Polym. Sci., Polym. Chem. Ed.*, vol. 23, no. 10, pp. 2683–2707, Oct. 1985, doi: 10.1002/pol.1985.170231011.

[10] L. Jensen, P.-O. Åstrand, A. Osted, J. Kongsted, and K. V. Mikkelsen, "Polarizability of molecular clusters as calculated by a dipole interaction model," *J. Chem. Phys.*, vol. 116, no. 10, pp. 4001–4010, Mar. 2002, doi: 10.1063/1.1433747.

[11] K. J. Miller, "Additivity methods in molecular polarizability," *J. Amer. Chem. Soc.*, vol. 112, no. 23, pp. 8533–8542, Nov. 1990, doi: 10.1021/ja00179a044.

[12] M. D. Hanwell, D. E. Curtis, D. C. Lonie, T. Vandermeersch, E. Zurek, and G. R. Hutchison, "Avogadro: An advanced semantic chemical editor, visualization, and analysis platform," *J. Cheminform.*, vol. 4, no. 1, p. 17, Aug. 2012, doi: 10.1186/1758-2946-4-17.

[13] M. C. Celina, "Review of polymer oxidation and its relationship with materials performance and lifetime prediction," *Polym. Degradation Stability*, vol. 98, pp. 2419–2429, Dec. 2013, doi: 10.1016/j.polymdegradstab.2013.06.024.

[14] S. Hettal, S. V. Suraci, S. Roland, D. Fabiani, and X. Colin, "Towards a kinetic modeling of the changes in the electrical properties of cable insulation during radio-thermal ageing in nuclear power plants. Application to silane-crosslinked polyethylene," *Polymers*, vol. 13, no. 24, p. 4427, Dec. 2021, doi: 10.3390/polym13244427.

[15] E. Linde, L. Verardi, D. Fabiani, and U. W. Gedde, "Dielectric spectroscopy as a condition monitoring technique for cable insulation based on crosslinked polyethylene," *Polym. Test.*, vol. 44, pp. 135–142, Jul. 2015, doi: 10.1016/j.polymertesting.2015.04.004.

[16] M. Ezzat, N. A. Sabiha, and M. Izzularab, "Accurate model for computing dielectric constant of dielectric nanocomposites," *Appl. Nanosci.*, vol. 4, no. 3, pp. 331–338, Mar. 2014, doi: 10.1007/s13204-013-0201-5.

[17] S. V. Suraci and D. Fabiani, "Aging modeling of low-voltage cables subjected to radio-chemical aging," *IEEE Access*, vol. 9, pp. 83569–83578, 2021, doi: 10.1109/ACCESS.2021.3086987.

[18] D. Fabiani and S. V. Suraci, "Broadband dielectric spectroscopy: A viable technique for aging assessment of low-voltage cable insulation used in nuclear power plants," *Polymers*, vol. 13, no. 4, p. 494, Feb. 2021, doi: 10.3390/polym13040494.

[19] S. V. Suraci, D. Fabiani, S. Roland, and X. Colin, "Multi scale aging assessment of low-voltage cables subjected to radio-chemical aging: Towards an electrical diagnostic technique," *Polym. Test.*, vol. 103, Nov. 2021, Art. no. 107352, doi: 10.1016/j.polymertesting.2021.107352.